FOLIA HISTOCHEMICA ET CYTOBIOLOGICA
Vol. 62, No. 2, 2023
pp. 109–122

ORIGINAL PAPER

VIA MEDICA

Cryptotanshinone ameliorates hemorrhagic shock-induced liver injury via activating the Nrf2 signaling pathway

Jiahui Han[1*], Di Jia[1*], Hao Yao[1], Ting Lv[2], Xi Xu[2], Xin Ge[1, 3]

[1]Department of ICU, Wuxi 9th People's Hospital Affiliated to Soochow University, Wuxi, Jiangsu 214000, P.R. China

[2]Department of ICU, Xishan People's Hospital of Wuxi City, Wuxi, Jiangsu, 214105, P.R. China

[3]Orthopedic Institution of Wuxi City, Wuxi, Jiangsu, 214000, P.R. China

[*]These authors contributed equally.

Abstract

Introduction. Hemorrhagic shock (HS) is an important cause of high mortality in traumatized patients. Cryptotanshinone (CTS) is a bioactive compound extracted from *Salvia miltiorrhiza* Bunge (Danshen). The current study aimed to explore the effect and underlying mechanism of CTS on the liver injury induced by HS.

Material and methods. Male Sprague-Dawley rats were used to establish the HS model by hemorrhaging and monitoring mean arterial pressure (MAP). CTS was intravenously administered at concentration of 3.5 mg/kg, 7 mg/kg, or 14 mg/kg 30 minutes before resuscitation. Twenty-four hours after resuscitation, the liver tissue and serum samples were collected for the following examinations. Hematoxylin and eosin (H&E) staining was used to evaluate hepatic morphology changes. The myeloperoxidase (MPO) activity in liver tissue and the serum activities of aspartate aminotransferase (AST) and alanine aminotransferase (ALT) were examined to reveal the extent of liver injury. The protein expression of Bax and Bcl-2 in liver tissue was detected by western blot. The TUNEL assay determined the apoptosis of hepatocytes. Oxidative stress of liver tissue was assessed by the examination of reactive oxygen species (ROS) generation. The content of malondialdehyde (MDA), glutathione (GSH), and adenosine triphosphate (ATP), the activity of superoxide dismutase (SOD) and oxidative chain complexes (complex I, II, III, IV), as well as cytochrome c expression in cytoplasm and mitochondria, were also used to determine the extent of oxidative injury in the liver. Immunofluorescence (IF) was employed to estimate nuclear factor E2-related factor 2 (Nrf2) expression. The mRNA and protein levels of heme oxygenase 1 (HO-1), NAD(P)H: quinone oxidoreductases 1 (NQO1), cyclooxygenase-2 (COX-2), and nitric oxide synthase (iNOS) were assessed by real-time qPCR, western blot to investigate the mechanism of CTS regulating HS-induced liver injury.

Results. H&E staining and a histological score of rat liver suggested that HS induced liver injury. The activity of ALT, AST, and MPO was significantly increased by HS treatment. After CTS administration the ALT, AST, and MPO activities were suppressed, which indicates the liver injury was alleviated by CTS. The HS-induced upregulation of the TUNEL-positive cell rate was suppressed by various doses of CTS. HS-induced ROS production was decreased and the protein expression of Bax and Bcl-2 in the HS-induced rat liver was reversed by CTS administration. In the liver of HS-induced rats, the upregulation of MDA content and the downregulation of GSH content and SOD activity

Correspondence addresses:
Dr. Xin Ge
Department of ICU, Wuxi 9th People's Hospital Affiliated to Soochow University, Wuxi, Jiangsu 214000, P.R. China
phone/fax: +86-510-85867999
e-mail: gexin2021@suda.edu.cn

Mr. Xi Xu
Department of ICU, Xishan People's Hospital of Wuxi City, Wuxi, Jiangsu 214105, P.R. China
e-mail: xuxi20221121icu@163.com

Folia Histochem Cytobiol. 2023
10.5603/FHC.a2023.0009
ISSN 0239-8508, e-ISSN 1897-5631

www.journals.viamedica.pl/folia_histochemica_cytobiologica

were suppressed by CTS. Additionally, CTS increases ATP content and mitochondrial oxidative complexes activities and suppressed the release of cytochrome c from mitochondria to the cytoplasm. Moreover, IF and western blot demonstrated that the activation of Nrf2 blocked by HS was recovered by different doses of CTS in liver tissue. The expression of downstream enzymes of the Nrf2 pathway, including HO-1, NQO1, COX-2, and iNOS, was reversed by CTS in the HS rat model.

Conclusions. The current study for the first time revealed the protective effect of CTS in HS-induced liver injury. CTS effectively recovered hepatocyte apoptosis, oxidative stress, and mitochondria damage induced by HS in the rat liver partly *via* regulating the Nrf2 signaling pathway. *(Folia Histochemica et Cytobiologica 2023, Vol. 61, No. 2, 109–122)*

Keywords: cryptotanshinone; *Salvia miltiorrhiza* Bunge; hemorrhagic shock; liver injury; ROS; Nrf2

Introduction

Hemorrhagic shock (HS) as an important cause of high mortality in traumatized patients [1] is a form of hypovolemic shock [2]. In severe cases, cellular hypoxia-induced cell damage results in multiple organ failure. This process is accompanied by oxidative stress, mitochondrial damage, inflammatory response, and apoptosis [3]. Due to the important role of the liver in metabolism and homeostasis, hemorrhagic shock (HS) disrupts hepatic cellular development and leads to liver dysfunction and injury [4–6]. The degree of liver damage is closely associated with mortality in traumatized patients [1]. Currently, effective treatment for HS is still required imminently [7]. Therefore, it is urgent to investigate the molecular mechanism of HS in the liver and to explore effective drugs for the treatment of liver injury.

Cryptotanshinone (CTS, CAS: 35825-57-1) is a diterpenoid compound extracted from *Salvia miltiorrhiza* Bunge that has been verified to resist oxidative stress, mitochondrial damage, and inflammatory response [8–10]. In recent years, CTS has attracted more and more attention as an effective anticancer substance [11]. Studies have revealed that CTS protects renal tubular epithelial cells from oxidative stress and apoptosis induced by hepatic ischemia/reperfusion (IR) [10]. Besides, CTS inhibits cardiomyocyte apoptosis induced by chronic hypoxia [12]. In addition, CTS could ameliorate the damage to placental and ovarian tissue *via* regulating oxidative stress, inflammation, and apoptosis [13, 14]. Moreover, it has been reported that the anti-inflammatory, antioxidant, and antifibrotic activities of CTS are mediated by the PI3K/Akt signaling pathway [15, 16]. However, the effect of CTS on HS-induced liver injury remains unclear. The present study explores the effect of CTS in the liver of rats subjected to HS and its possible mechanism.

Nuclear factor erythroid 2-related factor 2 (Nrf2) is an important transcription factor involved in the process of redox reactions. Excessive reactive oxygen species (ROS) production will activate the Nrf2 pathway, and the activation leads to a cascade reaction of antioxidative response element (ARE) in downstream genes [17, 18]. The activity of endogenous antioxidant enzymes, including heme oxygenase-1 (HO-1) and NAD(P)H: quinone oxidoreductases 1 (NQO1), can be further stimulated by the activation of Nrf2 in the cascade reactions of oxidative stress [19, 20]. The previous research showed that the Nrf2 pathway mediates the protective effects of herbal medicine on atherosclerosis [21]. The Nrf2 pathway can also be activated by oxyphylla A to alleviate neuropathology and ameliorate cognitive deficits in Alzheimer's murine models [22]. Moreover, the activation of the Nrf2 pathway has antioxidant and anti-inflammatory properties and contributes to the recovery of liver injury models [23–25]. It is still unknown whether the Nrf2 pathway is involved in the impact of CTS on liver injury.

In this study, we established rat model of HS-induced liver injury and resuscitation to identify the protective effects of CTS on hepatic injury and its mechanism. Results revealed that CTS effectively alleviated HS-induced liver injury, and inhibited hepatocyte apoptosis, oxidative stress, and mitochondria damage induced by HS through activating the Nrf2 pathway. This study provides powerful evidence for the effective therapeutic effect of CTS on liver injury in rats subjected to HS.

Material and methods

Establishment of a hemorrhagic shock rat model. Experiments were performed on male Sprague-Dawley rats (age 9 weeks, weight 275–325 g), which were free access to food and water in a comfortable environment with controlled temperature (21–23°C), humidity (45–55%) and lighting (12 h light/dark cycle). Before experiments, the rats were allowed to adapt to the environment for one week and then were fasted overnight, however, water was provided *ad libitum*. Before HS induction, the blood pressure value of rats was 103.7 ± ± 2.1 mmHg, which was measured on right femoral artery of rats using the BL420S physiological function experimental system (Techman Software, Chengdu, China). They were randomly divided into 5 groups, including a control group, HS group, HS + CTS 3.5 mg/kg group, HS + CTS 7 mg/kg group, and HS ± + CTS 14 mg/kg group. The establishment of a hemorrhagic

shock and resuscitation model was performed according to previous studies [26, 27]. Briefly, the left femoral artery was used for hemorrhaging, and the right femoral artery was used for monitoring mean arterial pressure (MAP) at 35–40 mmHg for 90 min. Rats were then resuscitated by shedding blood with Ringer lactate solution for 60 min. During this period, the rats received inhalation anesthesia of isoflurane. Subsequently, CTS (Aladdin, Shanghai, China) was dissolved in physiological saline to make solutions of different concentrations. Thirty minutes before the end of resuscitation, 1 mL of CTS (3.5, 7, or 14mg/kg) was intravenously injected into the rat tail. After 24 hours, we collected liver tissue samples of rats, and the blood samples from the inferior vena cava of rats. The blood samples were centrifuged at 3000 rpm for 10 min after 60 min rest at room temperature, and the supernatant (serum) was collected for subsequent analyses.

The chemical structure of CTS and experimental schedule were displayed in Fig. 1. This study was performed according to guidelines provided by the Animal Care Use Committee of Wuxi 9th People's Hospital Affiliated to Soochow University and was approved by the committee (Certificate No. KT2021026).

Histopathological analysis. Hepatic tissue was fixed in 4% paraformaldehyde and embedded in paraffin. The specimens were sliced into 5 μm sections and then dewaxed. Tissue slides were stained by hematoxylin (Solarbio, Beijing, China) and eosin (Sangon, Shanghai, China). The slides were observed using a BX53 microscope (Olympus, Tokyo, Japan) and were captured using the DP73 camera (Olympus, Tokyo, Japan). The grade of liver injury was assessed by histological score according to the standards described by El-Emam *et al.* [28]. One section per rat was evaluated in six animals per group. Three random fields were examined *per* slide and scores were averaged. A higher score implied more severe injury of liver tissue. Liver injury was scored according to the following changes of hepatocytes: (1) degree of fatty change and intracellular edema: 0 means none, 1 means mild, 2 means moderate, 3 means severe; (2) degree of vacuolation and necrosis: 0 means none, 1 means a few cells damage, 2 means submassive necrosis, 3 means massive necrosis and infarction. The sum of the two aspects is the histological score of liver injury.

Biochemical analysis. Myeloperoxidase (MPO) in liver tissue was detected using an MPO kit (Nanjing Jiancheng, Nanjing, China). Before detection, part of the liver tissue was weighted and homogenized in the prepared reagent II solution to gain 5% w/v homogenate. Tissues were homogenized using a glassy hand-pestled homogenizer on ice until they were completely homogenized. Then 0.9 mL homogenate and 0.1 mL reagent III solution were mixed, followed by warming in a 37°C water bath for 15 min. The same amount of mixture was mixed with reagent IV, chromogenic agent, and distilled water, and then reacted at 37°C for 30 min. After adding reagent VII and incubating at 60°C in a water bath for 10 min, the absorbance value of the mixture was immediately detected at 460 nm in a UV752N spectrophotometer (Yoke Instrument, Shanghai, China).

Collected liver tissue was weighed and added in physiological saline (0.9% NaCl) to obtain 10% (w/v) homogenate in an ice-cold water bath, and then centrifuged at 2500 rpm for 10 min. The supernatant was collected for the following assays. Malondialdehyde (MDA), glutathione (GSH), superoxide dismutase (SOD), and adenosine triphosphate (ATP) were measured using corresponding kits purchased from Nanjing Jiancheng Bioengineering Institute (Nanjing, China).

Liver tissue was homogenized in extract solution to get 10% (w/v) homogenate, which was then centrifuged at 600 × *g* for 10 min. The collected supernatant was transferred to another tube and centrifuged at 11000×*g* at 4°C for 15 min. Subsequently, extract solution was added to the sediment, and the mixture was sonicated with ultrasonic at 0°C (ultrasonic treatment for 5 s, intervals of 10 s, repeated 15 times). These samples were used to determine the activity of oxidative chain complexes (complex I, II, III, IV), which were examined using kits purchased from Solarbio Science and Technology (Beijing, China).

The generation of ROS in liver tissue was assessed using a frozen section ROS detection kit (BestBio, Shanghai, China). Fresh liver tissue was embedded with optimal cutting temperature compound (OCT) and pre-cooled on a frozen slicer. It was cut into 10 μm-thick slices. These liver sections were incubated with ROS fluorescent probe O13 solution at 37°C for 30 min. O13 is a fluorescent probe with cell membrane permeability. It is specifically oxidized by ROS to produce red fluorescence.

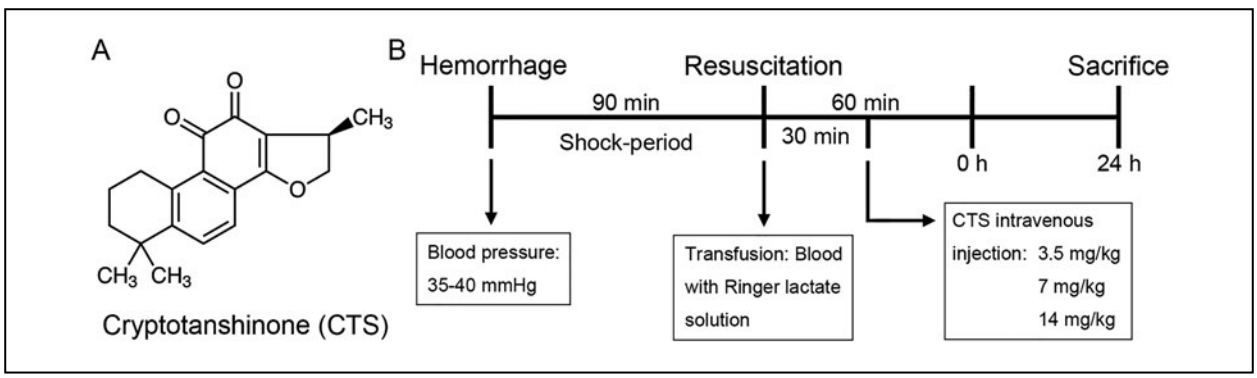

Figure 1. The information on cryptotanshinone (CTS) and model establishment. **A.** Chemical structure of CTS. **B.** The diagram of model establishment and experimental schedule.

Folia Histochem Cytobiol. 2023
10.5603/FHC.a2023.0009
ISSN 0239-8508, e-ISSN 1897-5631

The red fluorescence intensity corresponds to the level of ROS. The fluorescence was observed and captured using a BX53 microscope (Olympus, Tokyo, Japan).

Assessment of serum AST and ALT activity. The serum activities of aspartate aminotransferase (AST) and alanine aminotransferase (ALT) were evaluated using a Glutamic Oxalacetic transaminase (AST/GOT) kit and Alanine aminotransferase (ALT/GPT) kit (Wanleibio, Shenyang, China) separately.

Real-time qPCR. Total RNA was extracted from fresh liver tissue of the rats using TRIpure regent (BioTeke, Beijing, China) and was reverse-transcribed into cDNA using BeyoRT II M-MLV reverse transcriptase (Beyotime, Shanghai, China) following the manufacturer's instructions. Real-time qPCR was performed using 2 × Taq PCR Master Mix and SYBR Green (Solarbio, Beijing, China) to examine the mRNA expression of heme oxygenase-1 (HO-1), NAD(P)H: quinone oxidoreductases-1 (NQO-1), cyclooxygenase (COX)-2 and inducible nitric oxide synthase (iNOS), which was normalized by β-actin expression. The primers used in this part were listed as follows: HO-1 F: 5'-CATGTCCCAGGATTTGTC-3', R: 5'-GGGTTCTGCTTGTTTCG-3'; NQO1 F: 5'-GCCTACACGTATGCCACC-3', R: 5'-CCAGACGCTTCTTCCACC-3'; iNOS F: 5'-TTGGAGCGAGTTGTGGATTG-3', R: 5'-GTGAGGGCTTGCCTGAGTGA-3'; COX-2 F: 5'-GAACACGGACTTGCTCACTT-3', R: 5'-ACGATGTGTAAGGTTTCAGG-3'; β-actin F: 5'-GGAGATTACTGCCCTGGCTCCTAGC-3', R: 5'-GGCCGGACTCATCGTACTCCTGCTT-3'. Amplification was performed in Exicycler 96 Real-Time PCR system (Bioneer, Daejeon, Korea). The protocol used was as follows: denaturation at 94°C for 5 min, 40 cycles of 10 s at 94°C, 20 s at 60°C and 30 s at 72°C, followed by 2 min 30 s at 72°C, 1 min 30 s at 40°C, melting at 60°C to 94°C, every 1.0°C for 1 sec, 1–2 min at 25°C.

Western blot. Total protein was isolated from fresh liver tissue by RIPA lyase and PMSF (Beyotime, Shanghai, China). Following the instructions, a nuclear protein extraction kit (Beyotime, Shanghai, China) and a mitochondrial protein extraction kit (Boster, Wuhan, China) were used to extract nuclear protein and mitochondrial protein respectively. The concentration of protein was evaluated using a BCA protein assay kit (Beyotime, Shanghai, China). Proteins were separated by SDS-PAGE and transferred to polyvinylidene difluoride (PVDF) membranes (Thermo Fisher Scientific, PA, USA). After blocking for 1 h, membranes were incubated with primary antibodies overnight at 4°C and then were incubated with secondary antibodies for 40 min at 37°C. The blots were visualized by enhanced chemiluminescence substrate (7 Sea Biotech, Shanghai, China) and recorded using an imaging system (Beijing Liuyi, Beijing, China). The information on antibodies was listed in Table 1.

TUNEL assay. Cell apoptosis in the liver was examined using In Situ Cell Death Detection Kit (Roche, Basel, Switzerland). Briefly, the slides were permeabilized with 0.1% Triton X-100 (Beyotime, Shanghai, China) for 8 min at room temperature. Subsequently, the TUNEL reaction solution was added to the slides and incubated for 60 min at 37°C in the dark. After being washed with phosphate buffer saline (PBS), the slides were counterstained by DAPI (Aladdin, Shanghai, China) for 5 min in the dark.

Immunofluorescence of Nrf2. Liver tissue slides were treated with antigen retrieval solution (pH = 6.0) at 60–80°C for 10 min. The sections were incubated with Nrf2 antibody (dilution 1: 100, AF0639, Affinity, Changzhou, China) overnight at 4°C, and then were incubated with Cy3 labeled Goat anti-rabbit IgG (dilution 1: 200, A27039, Invitrogen, CA, USA) for 60 min. Then, DAPI was used to redye cell nuclei after PBS washing. The expression of Nrf2 was observed by immunofluorescence (IF) under a BX53 microscope (Olympus, Tokyo, Japan).

Statistical analysis. All statistical analyses were performed using GraphPad Prism 8.0 (GraphPad Software, San Diego,

Table 1. The information of antibodies used for western blot

Name	Catalog number	Dilution	Company
Bax	A19684	1:500	ABclonal
Bcl-2	A0208	1:500	ABclonal
Cytochrome C	12245-1-AP	1:500	Proteintech
HO-1	A19062	1:1000	ABclonal
NQO1	A19586	1:1000	ABclonal
COX-2	A3560	1:1000	ABclonal
iNOS	A0312	1:500	ABclonal
Nrf2	A1244	1:1000	ABclonal
β-actin	60008-1-Ig	1:2000	Proteintech
COX IV	A11631	1:500	ABclonal
Histone H3	17168-1-AP	1:500	Proteintech
Goat anti-Rabbit IgG	SA00001-2	1:10000	Proteintech
Goat anti-Mouse IgG	SA00001-1	1:10000	Proteintech

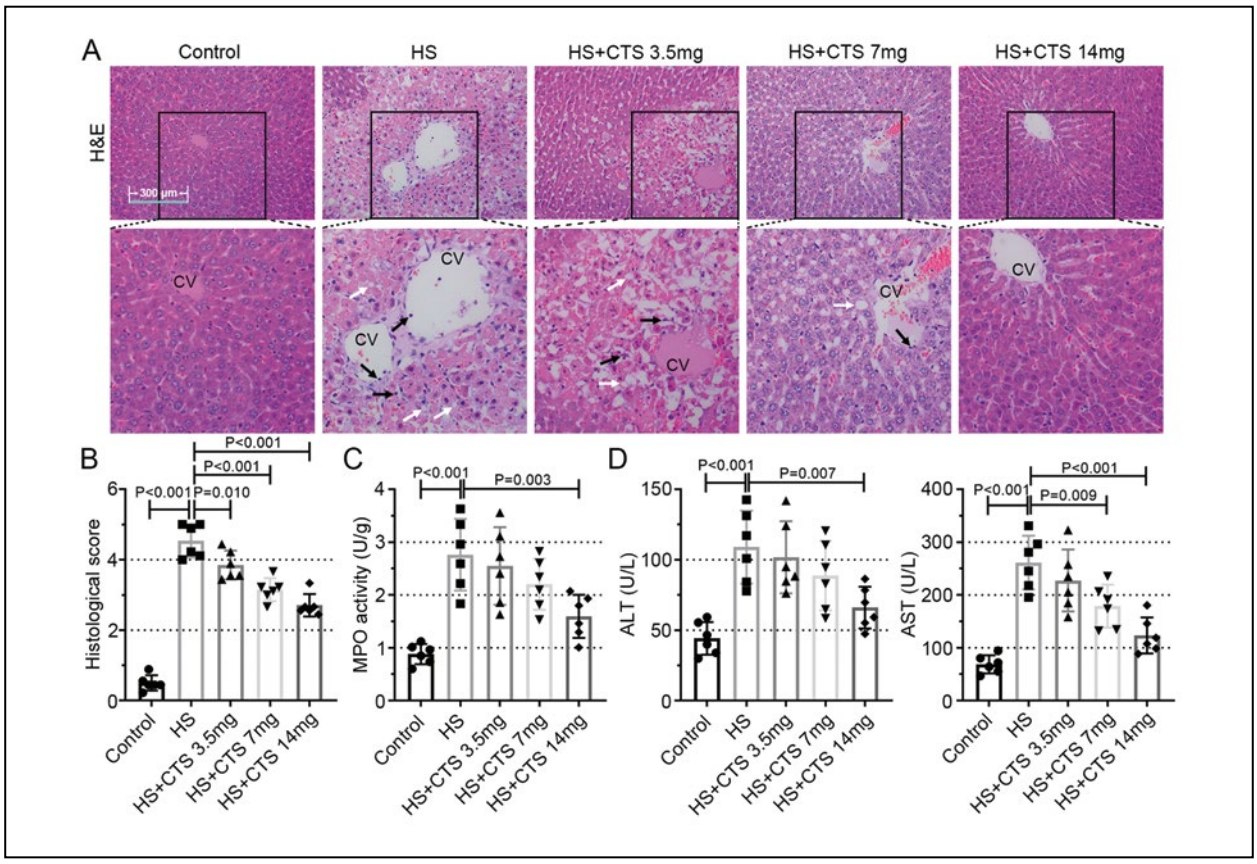

Figure 2. CTS ameliorates hemorrhagic shock (HS)-induced liver injury. **A.** The liver injury was evaluated by hematoxylin and eosin staining of liver sections (CV: central vein and sublobular vein; black arrows: hepatocyte necrosis; white arrows: hepatocyte vacuolation). Scale bar: 300 μm. **B.** The histopathological scores of liver injury in different groups. **C.** The myeloperoxidase (MPO) activity of liver tissue was assessed as described in Methods. **D.** The activities of aspartate aminotransferase (AST) and alanine aminotransferase (ALT) in the rat serum were measured as described in Methods. Data are shown as mean ± SD, n = 6 for each group.

CA, USA). The results were presented as mean ± standard deviation (SD). All our results were tested for homogeneity of variance. Statistical differences among different groups were analyzed by one-way ANOVA followed by Dunnett's multiple comparisons tests. The results with inconsistent variance were analyzed by the Kruskal-Wallis test. $P < 0.05$ was considered statistically significant.

Results

CTS ameliorates hepatic injury induced by hemorrhagic shock

Histopathological examination of liver sections in the control group showed that hepatic lobule structure was complete and hepatocytes were regularly arranged. The incomplete structure of the hepatic lobule was observed in the HS group, and necrosis, and vacuolation occurred in hepatocytes. After treatment with different concentrations of CTS treatment, liver injury presented various degrees of recovery from the HS--induced injury (Fig. 2A). The H&E-stained sections and data from each rat are shown as Supplementary Figures S1–S5. The histopathological scores suggested that HS significantly induced the injury, and CTS treatment remarkably suppressed the damage of liver tissues induced by HS (Fig. 2B). Additionally, MPO activity was dramatically raised by HS in rat liver, and was remarkably suppressed by the treatment with 14 mg/kg CTS. The high dose of CTS was associated with a significant decrease of MPO activity in liver tissue (Fig. 2C). Serum ALT and AST activities as crucial indicators of liver injury [29] were highly increased by HS. The 7 mg/kg CTS treatment resulted in a marked decrease in serum AST, and 14 mg/kg CTS significantly downregulated serum ALT and AST (Fig. 2D). These findings confirmed the protective role of CTS against liver injury induced by HS *in vivo*.

CTS suppresses hemorrhagic shock-induced hepatic cell apoptosis

Subsequently, we investigated the effects of CTS on HS-induced cell apoptosis in the liver tissue of the rat model. As shown in Fig. 3A, the number of TUNEL--positive liver cells was remarkably increased in the HS group. The results of statistical analysis showed

Folia Histochem Cytobiol. 2023
10.5603/FHC.a2023.0009
ISSN 0239-8508, e-ISSN 1897-5631

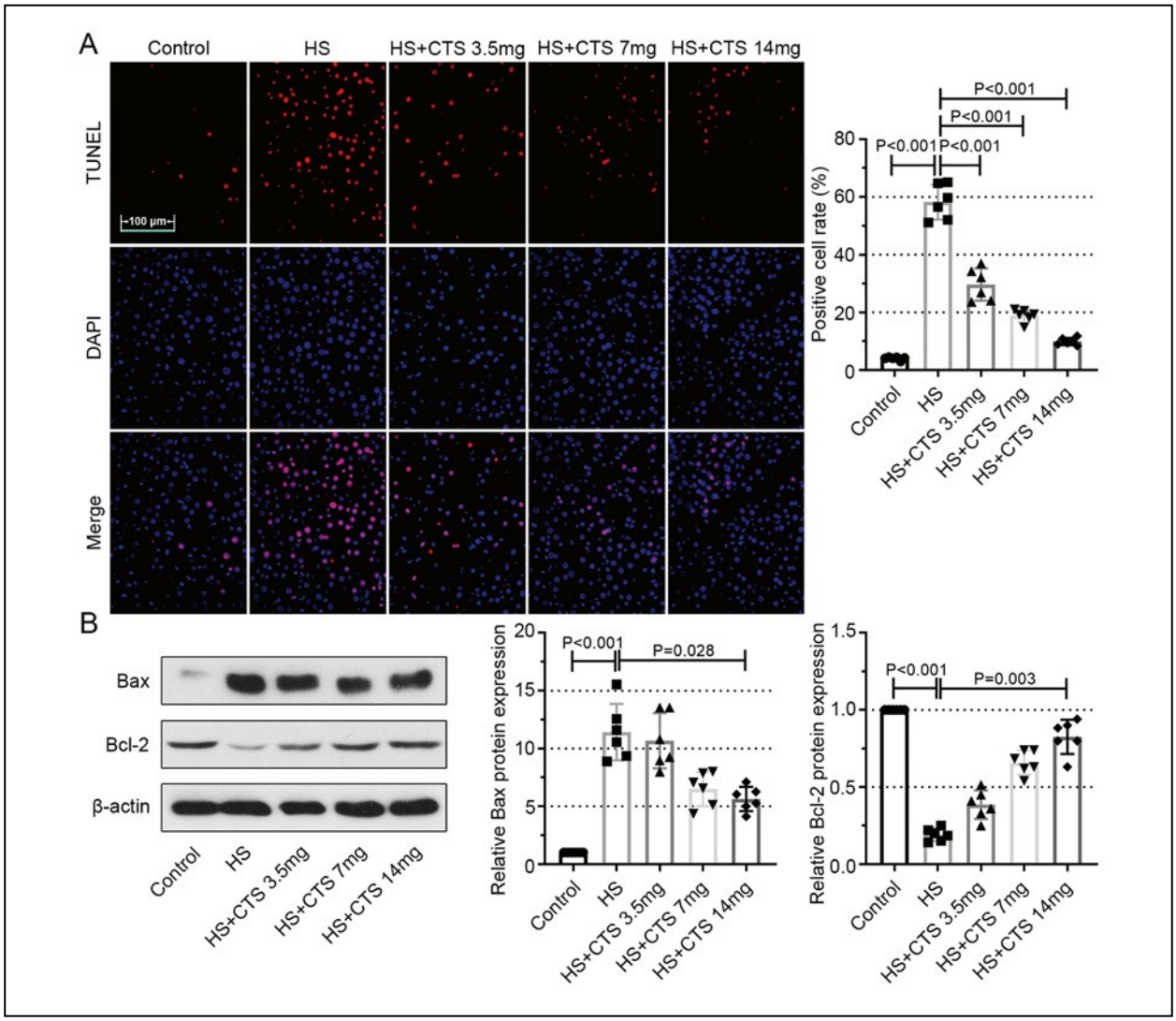

Figure 3. CTS inhibits HS-induced hepatic cell apoptosis. **A.** The hepatocyte apoptosis was examined in liver sections by TUNEL staining as described in Methods. Cell nuclei were stained by DAPI. Scale bar: 100 μm. **B.** The protein expression of Bax and Bcl-2 in the liver tissue was measured by western blot. Data are shown as mean ± SD, n = 6 for each group.

that various doses of CTS effectively suppressed hepatocyte apoptosis. Western blot results exhibited that the protein expression of apoptotic gene *Bax* was increased and the antiapoptotic gene *Bcl-2* was reduced in the liver of HS-treated rats. With the increase of CTS concentration, Bax expression was suppressed and Bcl-2 expression was enhanced in liver tissue (Fig. 3B). The above findings proved that CTS inhibited the hepatocyte apoptosis induced by HS in rat liver.

CTS protects the liver from oxidative stress induced by hemorrhagic shock

As displayed in Fig. 4A, the production of ROS was dramatically upregulated in the liver tissue of the HS rat model. CTS blocked the excessive ROS production and suppressed the oxidative stress in the liver. The increase of MDA content induced by HS was significantly reduced by 14 mg/kg CTS treatment (Fig. 4B). The GSH content was decreased in the liver tissue under HS condition, and it was rescued by the treatment with 14 mg/kg CTS. Meanwhile, HS-induced downregulation of SOD activity was dramatically reversed by 7 mg/kg and 14 mg/kg CTS (Fig. 4C). These findings indicated that CTS attenuated the oxidative stress induced by HS in liver tissue.

CTS attenuates hemorrhagic shock-induced mitochondrial damage in liver tissue

Previous studies have demonstrated that HS reduced the production of mitochondrial ATP and the activities of respiratory chain complexes, and increased the release of cytochrome c into cytoplasm in animal models, indicating the mitochondria were damaged [30–32]. As depicted in Fig. 5A, the activity of complexes

10.5603/FHC.a2023.0009
ISSN 0239-8508, e-ISSN 1897-5631

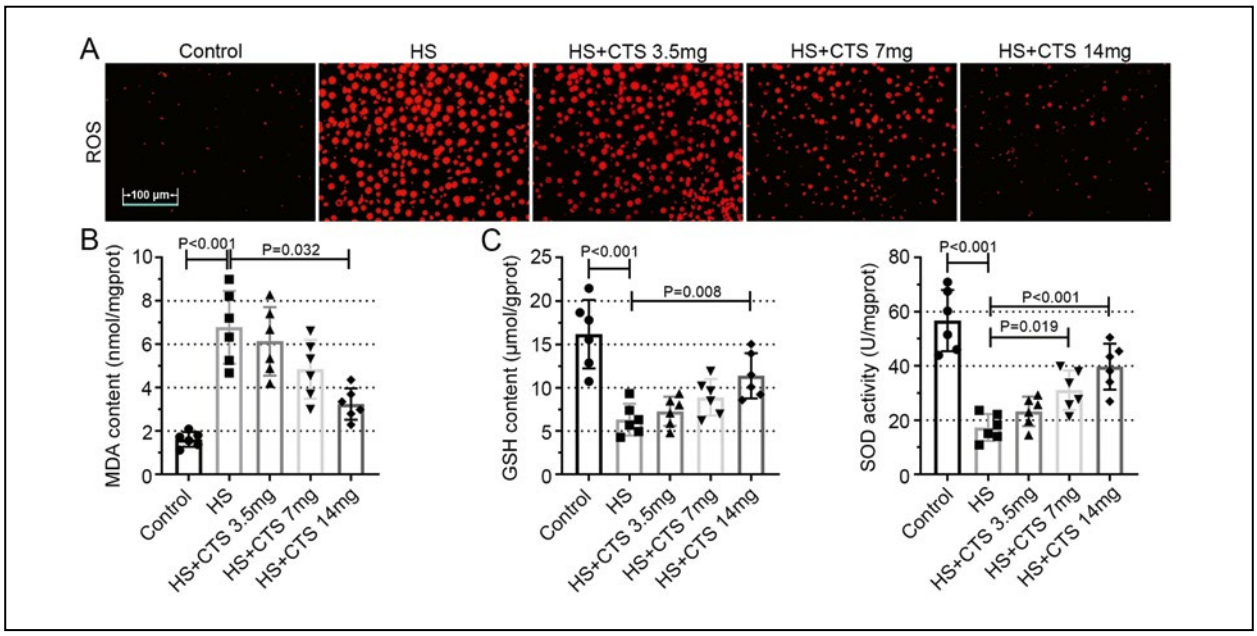

Figure 4. CTS protects against oxidative stress in liver tissue of HS-induced rats. **A.** The generation of reactive oxygen species (ROS) was detected by staining liver sections with a sensitive fluorescent probe O13. Scale bar: 100 μm. **B, C.** The malondialdehyde (MDA), glutathione (GSH) content, and superoxide dismutase (SOD) activity were determined in the liver. Data are shown as mean ± SD, n = 6 for each group.

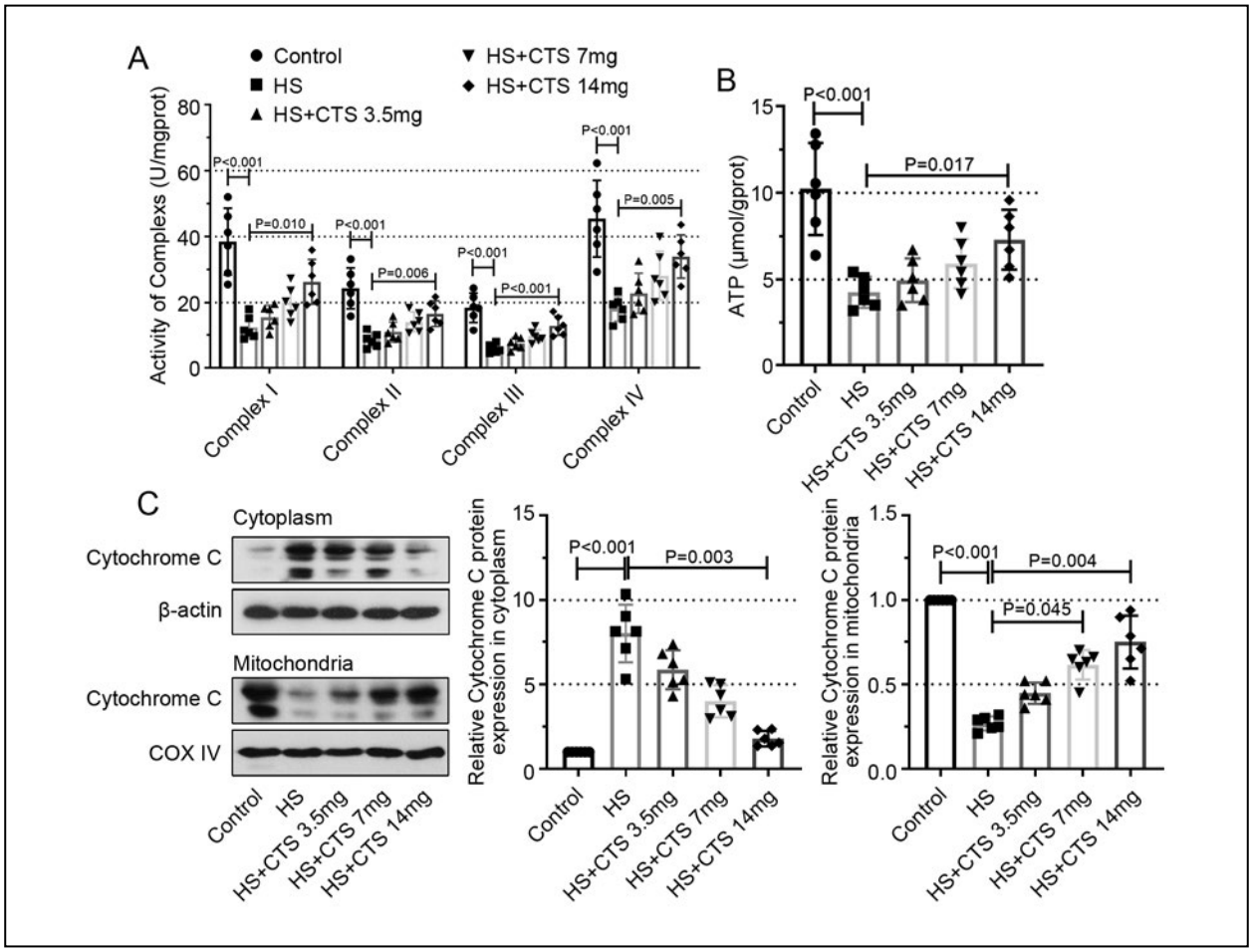

Figure 5. CTS attenuates HS-induced mitochondrial damage in liver tissue. **A, B.** The oxidative chain activities (complexes I–IV) and adenosine triphosphate (ATP) generation were evaluated in rat liver as described in Methods. **C.** The protein expression of cytochrome c in the cytoplasm and in mitochondria was examined by western blot. Data are shown as mean ± SD, n = 6 for each group.

Folia Histochem Cytobiol. 2023
10.5603/FHC.a2023.0009
ISSN 0239-8508, e-ISSN 1897-5631

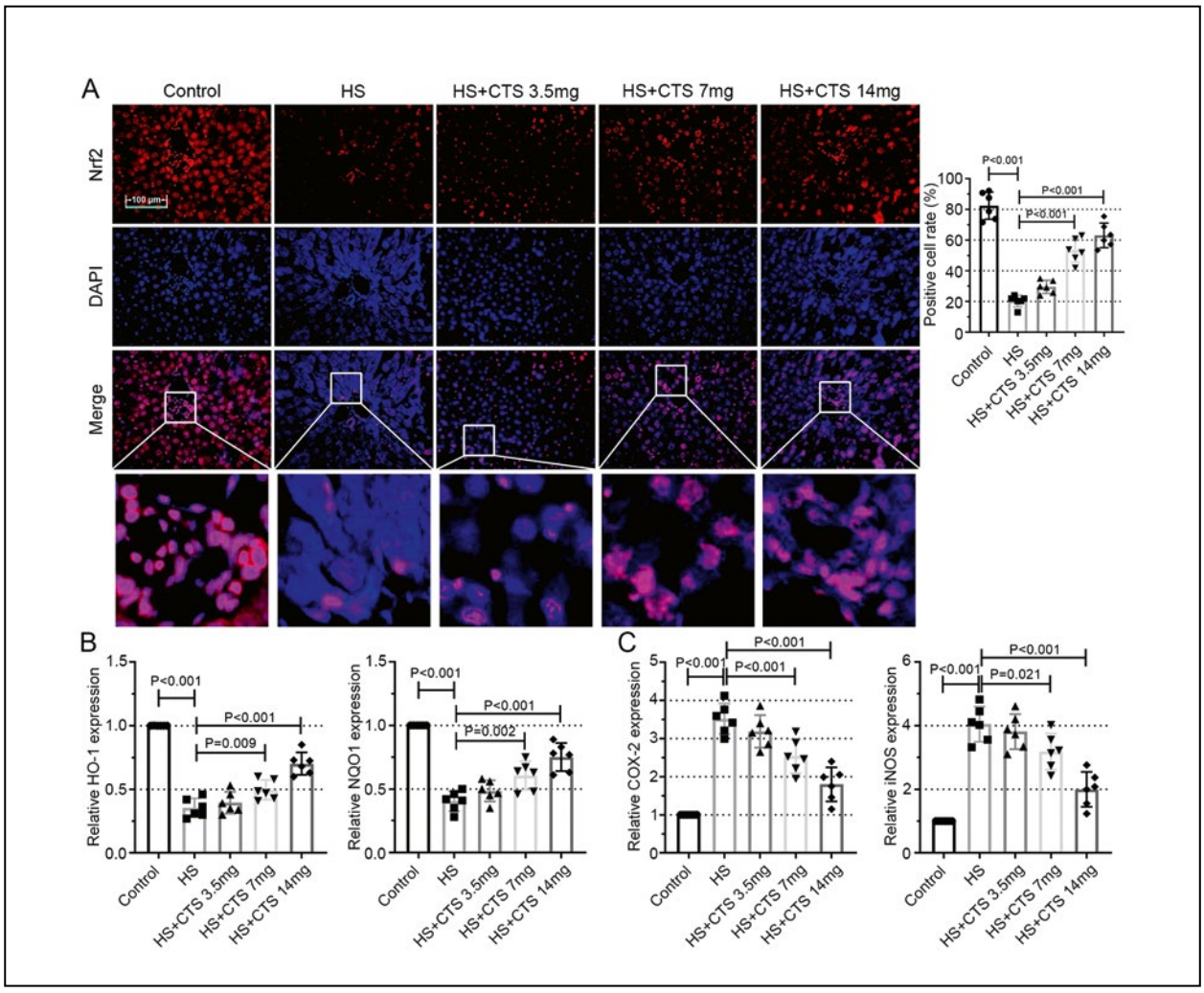

Figure 6. CTS activates the nuclear factor E2-related factor 2 (Nrf2) pathway. **A.** The expression and distribution of Nrf2 were evaluated by immunofluorescence (IF) in liver sections. Scale bar: 100 μm. **B, C.** The relative mRNA levels of heme oxygenase 1 (HO-1), NAD(P)H: quinone oxidoreductases 1 (NQO1), cyclooxygenase-2 (COX-2), and nitric oxide synthase (iNOS) were measured by RT-qPCR. Data are shown as mean ± SD, n = 6 for each group.

(complex I, II, III, and IV) was remarkably down-regulated in the liver of the HS group. With the increased doses of CTS, the activity of complexes was upregulated and was significantly raised by 14 mg/kg CTS. Besides, the mitochondrial ATP production was significantly decreased in the liver of HS-induced rats. Meanwhile, the increased concentration of CTS upregulated the ATP level in the liver (Fig. 5B). Moreover, western blot results indicated that cytochrome c expression was increased in the cytoplasm and decreased in mitochondria of hepatocytes induced by HS, while these changes were significantly reversed in rats that received various doses of CTS (Fig. 5C). These phenomena indicated that CTS attenuated mitochondrial damage in liver tissue of HS rat model.

The Nrf2 pathway mediates the effects of CTS on hemorrhagic shock-induced liver injury

The follow-up experiments were performed to explore whether Nrf2 mediates the effect of CTS on liver injury in the HS rat model. IF results suggested the activation of Nrf2 was significantly blocked in the liver tissue of the HS rat model compared with the control group. After being treated with different doses of CTS, the expression of Nrf2 in the nucleus was increased in liver tissue (Fig. 6A). The mRNA levels of HO-1 and NQO1 were markedly reduced in the liver tissue of the HS rat model, and were significantly up-regulated by CTS (Fig. 6B). Meanwhile, the upregulation of COX-2 and iNOS induced by HS was suppressed by various doses of CTS (Fig. 6C). These results illustrated that the Nrf2 pathway was activated by CTS in HS rat model.

Folia Histochem Cytobiol. 2023
10.5603/FHC.a2023.0009
ISSN 0239-8508, e-ISSN 1897-5631

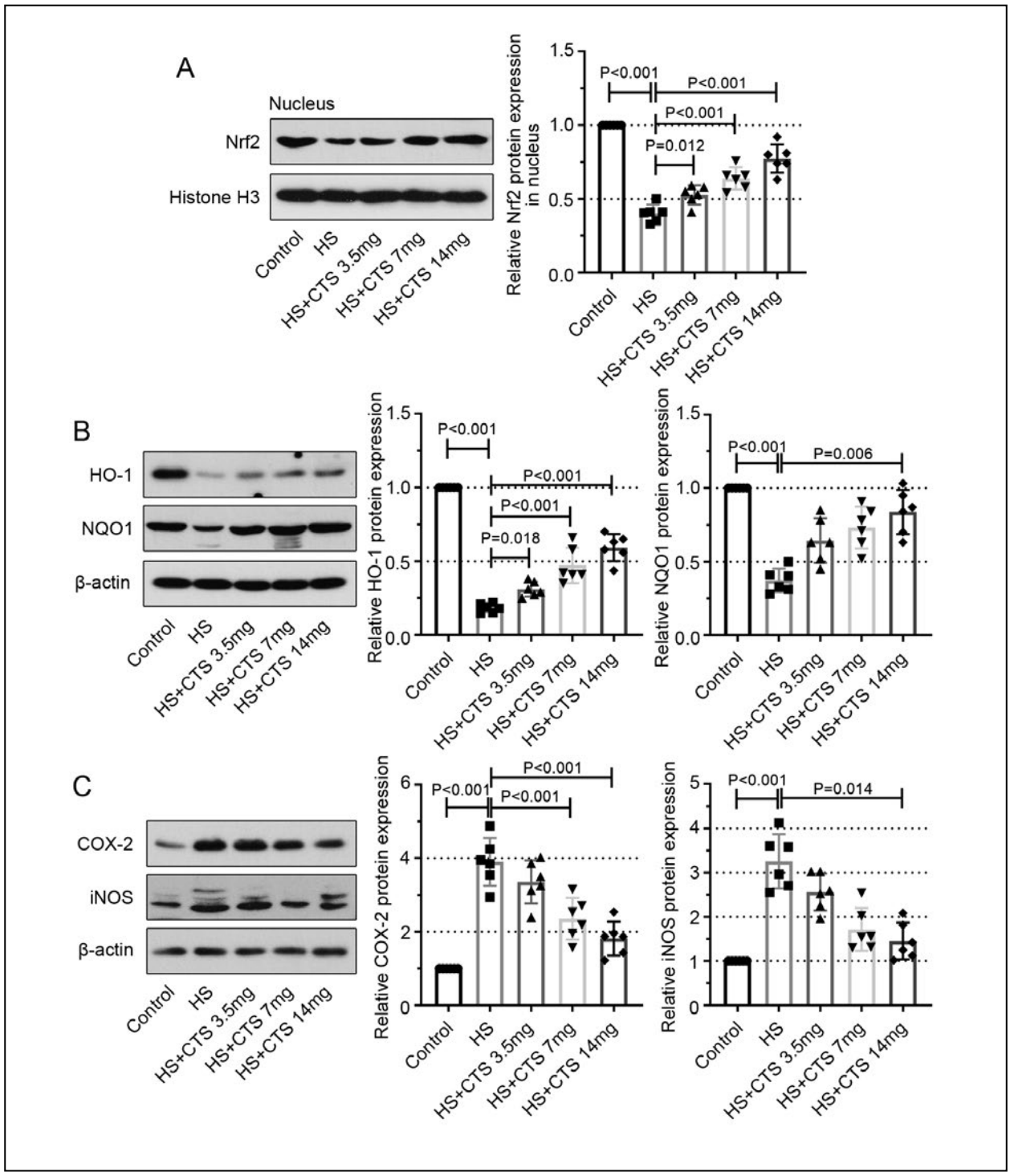

Figure 7. The effect of CTS on the protein expression of Nrf2, HO-1, NQO1, COX-2, and iNOS. **A.** The nuclear Nrf2 expression in the nucleus was examined using a western blot. **B, C.** The protein levels of HO-1, NQO1, COX-2, and iNOS were determined in the liver by western blotting. Data are shown as mean ± SD, n = 6 for each group.

Furthermore, the protein expression of Nrf2 in the nucleus was obviously decreased in the HS group compared with the control group. CTS activated Nrf2 expression and promoted the transfer of Nrf2 from the cytoplasm to the nucleus (Fig. 7A). Additionally, HO-1 and NQO1 were obviously decreased in the HS rat model. The treatment of CTS remarkably upregulated the expression of HO-1 and NQO1 (Fig. 7B). In Fig. 7C, the protein expression of COX-2 and iNOS was induced in HS rat model and was declined by different dosages of CTS. The above findings further demonstrated that CTS can activate the Nrf2 pathway.

Folia Histochem Cytobiol. 2023
10.5603/FHC.a2023.0009
ISSN 0239-8508, e-ISSN 1897-5631

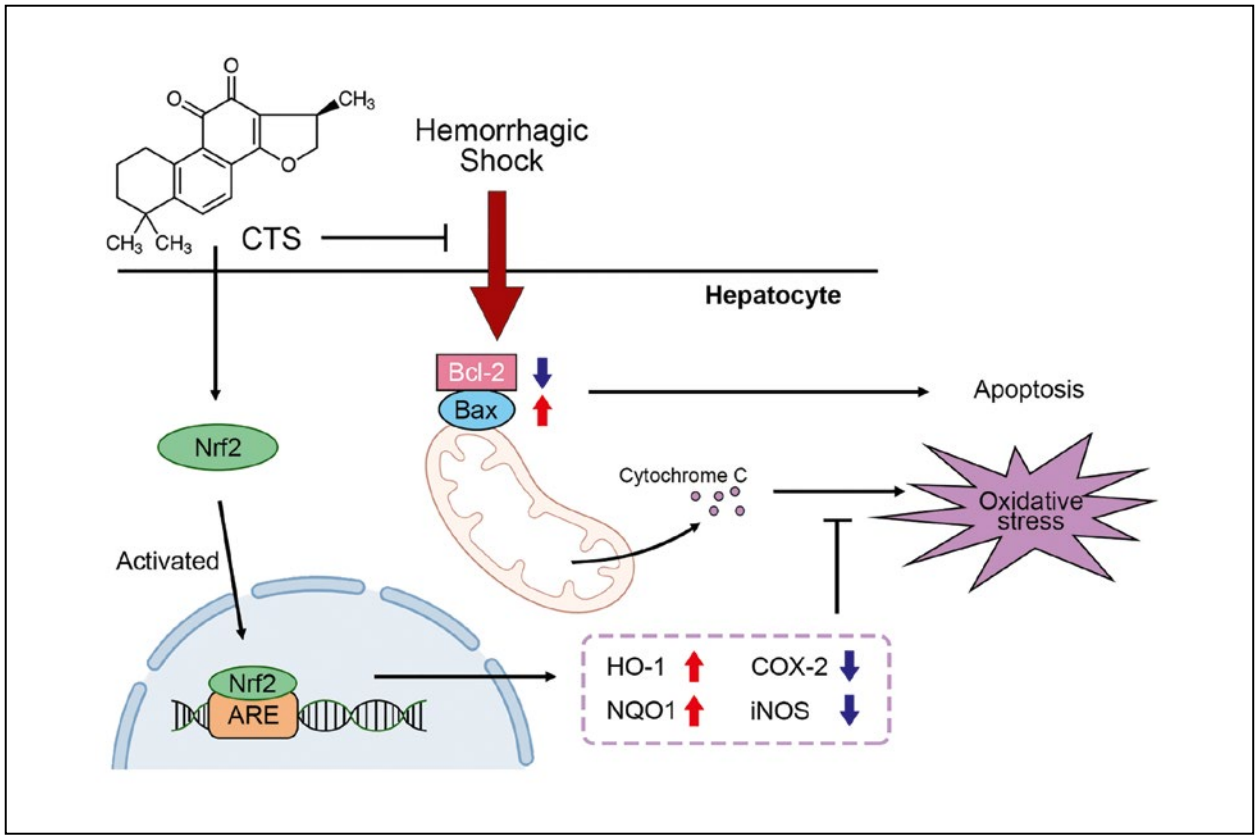

Figure 8. Molecular mechanism of CTS in rescuing HS-induced liver injury as described in the Discussion.

Discussion

The protective effect of CTS on the liver injury induced by hemorrhagic shock was confirmed in the present study. The liver injury-related parameters, including MPO activity, AST and ALT concentrations, and hepatocyte morphology were recovered by different concentrations of CTS. CTS effectively suppressed the increase of Bax expression and decrease of Bcl-2 expression induced by HS, which suggested that CTS reversed the HS-induced hepatocyte apoptosis. Meanwhile, CTS inhibited HS-induced oxidative stress and mitochondrial damage by activating the Nrf2 to enhance the expression of HO-1 and NQO1, as well as reducing the expression of COX-2 and iNOS (Fig. 8). Thus, the results of our study indicate that may serve as a potential therapeutic agent for ameliorating HS-induced liver injury.

It is well-known that Chinese herbal medicine plays an effective role in various diseases due to its multiple bioactive substances [15]. CTS is one of the main active components of the traditional Chinese medicine Danshen, which has been widely used in the treatment of various disorders [11]. Till now, CTS has not been studied in a rat model of hemorrhagic shock. Since hemorrhagic shock is an acute disease, we planned to use intravenous injections to promote the effect of CTS in this study. In a study of cerebral ischemia-reperfusion injury, which is also an acute disease, CTS was intravenously administered at a concentration of 10 mg/kg for 0.5 h in a mouse model to ameliorate the injury [33]. After conversion by the surface area method, we determined a dose of 7 mg/kg for rats. Besides, CTS was found to improve type 2 diabetes and obesity in a dose-dependent manner [9]. Based on the information, the dosages of CTS were determined to be 3.5 mg/kg, 7 mg/kg, and 14 mg/kg in this study. During the study, the rats did not exhibit abnormality or discomfort signs, so the dose of CTS was considered to be safe for rats. To the best of our knowledge, CTS has not been reported in clinical research. The current study preliminarily revealed the alleviative effect of CTS on HS-induced liver injury. The security, dosage, and mechanism of CTS will be the important contents of our follow-up research, which aims to provide a more experimental basis for the clinical application of CTS.

In recent decades, increasing research have revealed the molecular and pathological mechanisms of CTS in a variety of diseases. For example, CTS suppressed the development of breast cancer by activating GPER to downregulate the PI3K/AKT signaling pathway [15]. Besides, CTS protected ovarian tissue from polycystic ovary syndrome induced damage [14]. Moreover, the ischemia/reperfusion induced neurotoxicity and acute kidney injury were both ameliorated by the treatment of CTS [10, 33].

Folia Histochem Cytobiol. 2023
10.5603/FHC.a2023.0009
ISSN 0239-8508, e-ISSN 1897-5631

Our study further identified the therapeutic effects of CTS on liver injury induced by HS. In the HS rat model, the necrosis, vacuolation, and infiltration occurred in hepatocytes and the hepatic MPO, and serum ALT and AST activities increased abnormally. The treatment of CTS in higher concentrations effectively alleviated the above phenomenon. In the preliminary stage of the study, we found that most of the researchers used male animals to build this model [26, 27, 34–36], thus we speculate that there may be no gender difference in HS-induced liver injury. In addition, there are hormonal changes in the physiological cycle of female rats and mice, thus, in order to avoid the uncontrollable factors, we chose male rats for modeling. Our study demonstrated the ameliorative effect of CTS on HS-induced liver injury.

Hemorrhagic shock remains a common and dangerous condition in traumatic patients. For the liver, a crucial organ controlling body's metabolism, HS will lead to metabolic disorders, serious damage or even organ failure [37]. In this study, the liver injury induced by HS was accompanied by oxidative stress, mitochondrial damage, and apoptosis of liver cells. It is well known that Bax as an inactive monomer is present in the cytoplasm under normal condition and the Bcl-2 family proteins maintain the mitochondrial integrity [38, 39]. These proteins regulate the release of cytochrome c and the intrinsic pathway of apoptosis [40]. Following the ischemia–hypoxia stimulus, the activated and upregulated Bax changes the structure of specific membrane proteins to allow the release of cytochrome c from the mitochondrion to the cytoplasm [41], which is similar to the findings of our research. The mitochondrial apoptosis-induced channel regulated by Bcl-2 family proteins might control the activation of Bax [42]. In our study, we verified that in the TUNEL-positive cells, the expression of Bax and cytochrome c in the cytoplasm were increased by HS treatment, and the expression of Bcl-2 and mitochondrial membrane potentials were decreased, indicating that the mitochondrial damage and hepatic cell apoptosis were induced by HS. Additionally, the primary function of mitochondria is ATP production, which is executed by the respiratory chain complexes (I, II, III, and IV) [43]. The levels of ATP and activity of respiratory chain complexes were significantly downregulated in the liver tissue of HS-induced rats. The CTS treatment remarkably rescued these changes and improved the expression of Bax, Bcl-2, ATP, complexes, and cytoplasmic cytochrome c to the normal level, resulting in the recovery of the mitochondrial damage and hepatic cell apoptosis.

The Nrf2 pathway was shown to have hepatoprotective effects in toxic hepatitis [4]. The activation of Nrf2 has been reported to be beneficial in the models of liver injury caused by different causes [23, 24, 44, 45]. The Nrf2 as a member of the basic region of the leucine zipper (bZIP) transcription factor family interacts with Kelch-like ECH-associated protein 1 (Keap1), leading to the suppression of Nrf2 activation [46]. After dissociating from Keap1, Nrf2 transfers into the nucleus and then interacts with the ARE of downstream genes, mediating the expression of some antioxidant enzymes, including HO-1 and NQO1 [47]. The HO-1 and NQO1 regulated by the activation of Nrf2 exert antioxidant and anti-inflammatory activities [48, 49]. The Nrf2 was shown to significantly alleviate liver injury, while the silencing of Nrf2 aggravated oxidative stress and inflammation of liver tissue [50]. The activation of the Nrf2 pathway was found to reduce oxidative stress, further resulting in the alleviation of liver injury [4]. A previous study has indicated that the Nrf2 pathway agonist exerts anti-inflammatory effects by blocking the expression of TNF-α, COX-2, and iNOS [51, 52]. Upregulation of COX-2 and iNOS was found in damaged cells [53]. In line with these findings, our results suggest that the expression of Nrf2 was suppressed in the liver of HS-induced rats and was downregulated in the cell nuclei. In this context, mRNA and protein expression of HO-1 and NQO1 were both significantly decreased, indicating the promotion of the oxidative stress that was confirmed by the increase of MDA and the decrease of GSH contents, and suppression of SOD activity. Meanwhile, the mRNA and protein expression of COX-2 and iNOS were upregulated, indicating that HS induced the inflammatory reaction of the liver tissue. Serum AST and ALT activities, useful indicators of hepatic injury, were upregulated in HS-induced liver. The administration of CTS activated the Nrf2 pathway and upregulated the expression of Nrf2 in the nucleus. All these markers of oxidative stress, inflammatory and hepatic injury were rescued by CTS treatment. These findings prove that CTS could effectively protect liver tissue and hepatocytes from the injury induced by HS *via* activating the Nrf2 pathway.

Hemorrhagic shock is an acute lesion with predominantly renal injury in the early stages and widespread multiorgan failure and multiorgan insufficiency, including liver and cardiovascular injury, in the middle and advanced stages [54, 55]. While Nrf2 is an important anti-inflammatory and antioxidant factor, inhibition of Nrf2 or Nrf2-knockdown will exacerbate damage to a variety of organs and cause higher mortality [56–58]. We speculate that this is also the reason why Nrf2 inhibitors are rarely used *in vivo* for HS-related studies.

In conclusion, cryptotanshinone ameliorates oxidative stress, mitochondrial damage, and hepatic cell apoptosis in the liver of rats subjected to hemorrhage shock and resuscitation. CTS may protect the liver from HS-induced injury partly by the activation of the Nrf2 pathway.

Acknowledgments

Not applicable.

Folia Histochem Cytobiol. 2023
10.5603/FHC.a2023.0009
ISSN 0239-8508, e-ISSN 1897-5631

Funding

This research was supported by the Major Scientific Projects of Wuxi Municipal Healthy Commission (grant no. Z202105), the Science and Technology Development Fund Project of Wuxi (grant no. Y20212057), and the Wuxi Top Medical Expert Team of "Taihu Talent Program".

Conflict of interest

The authors declare that there is no conflict of interest.

Author's statement

The work has not been submitted for publication elsewhere.

Author contributions

This study was designed by Xi Xu and Xin Ge. Data collection and analysis were performed by Jiahui Han, Di Jia, Hao Yao, and Ting Lv. The manuscript was drafted by Jiahui Han and Di Jia, and all authors contributed to the revision of the manuscript. All authors approved the final manuscript and agreed to be accountable for all aspects of this study.

Supplementary materials

Supplementary materials are available on journal's website.

References

1. Eastridge BJ, Holcomb JB, Shackelford S, et al. Outcomes of traumatic hemorrhagic shock and the epidemiology of preventable death from injury. Transfusion. 2019; 59(S2): 1423–1428, doi: 10.1111/trf.15161, indexed in Pubmed: 30980749.
2. Cannon JW, Cannon JW. Hemorrhagic Shock. N Engl J Med. 2018; 378(4): 370–379, doi: 10.1056/NEJMra1705649, indexed in Pubmed: 29365303.
3. Chen H, Huang RS, Yu XX, et al. Emodin protects against oxidative stress and apoptosis in HK-2 renal tubular epithelial cells after hypoxia/reoxygenation. Exp Ther Med. 2017; 14(1): 447–452, doi: 10.3892/etm.2017.4473, indexed in Pubmed: 28672952.
4. Liang W, Greven J, Qin K, et al. Sulforaphane exerts beneficial immunomodulatory effects on liver tissue via a Nrf2 pathway-related mechanism in a murine model of hemorrhagic shock and resuscitation. Front Immunol. 2022; 13: 822895, doi: 10.3389/fimmu.2022.822895, indexed in Pubmed: 35222401.
5. Liu H, Xiao X, Sun C, et al. Systemic inflammation and multiple organ injury in traumatic hemorrhagic shock. Front Biosci (Landmark Ed). 2015; 20(6): 927–933, doi: 10.2741/4347, indexed in Pubmed: 25961533.
6. Matot I, Katz M, Pappo O, et al. Resuscitation with aged blood exacerbates liver injury in a hemorrhagic rat model. Crit Care Med. 2013; 41(3): 842–849, doi: 10.1097/CCM.0b013e3182711b38, indexed in Pubmed: 23314580.
7. Guan Z, Zhou L, Zhang Yu, et al. Sulforaphane ameliorates the liver injury of traumatic hemorrhagic shock rats. J Surg Res. 2021; 267: 293–301, doi: 10.1016/j.jss.2021.05.004, indexed in Pubmed: 34174694.
8. Jin YC, Kim CW, Kim YM, et al. Cryptotanshinone, a lipophilic compound of Salvia miltiorrriza root, inhibits TNF-alpha-induced expression of adhesion molecules in HUVEC and attenuates rat myocardial ischemia/reperfusion injury in vivo. Eur J Pharmacol. 2009; 614(1-3): 91–97, doi: 10.1016/j.ejphar.2009.04.038, indexed in Pubmed: 19401198.
9. Kim EJu, Jung SN, Son KHo, et al. Antidiabetes and antiobesity effect of cryptotanshinone via activation of AMP-activated protein kinase. Mol Pharmacol. 2007; 72(1): 62–72, doi: 10.1124/mol.107.034447, indexed in Pubmed: 17429005.
10. Zhu R, Wang W, Yang S, et al. Cryptotanshinone inhibits hypoxia/reoxygenation-induced oxidative stress and apoptosis in renal tubular epithelial cells. J Cell Biochem. 2019; 120(8): 13354––13360, doi: 10.1002/jcb.28609, indexed in Pubmed: 30891815.
11. Wu YH, Wu YR, Li Bo, et al. Cryptotanshinone: A review of its pharmacology activities and molecular mechanisms. Fitoterapia. 2020; 145: 104633, doi: 10.1016/j.fitote.2020.104633, indexed in Pubmed: 32445662.
12. Jin HJ, Xie XL, Ye JM, et al. TanshinoneIIA and cryptotanshinone protect against hypoxia-induced mitochondrial apoptosis in H9c2 cells. PLoS One. 2013; 8(1): e51720, doi: 10.1371/journal.pone.0051720, indexed in Pubmed: 23341883.
13. Wang Na, Dong X, Shi D, et al. Cryptotanshinone ameliorates placental oxidative stress and inflammation in mice with gestational diabetes mellitus. Arch Pharm Res. 2020; 43(7): 755–764, doi: 10.1007/s12272-020-01242-1, indexed in Pubmed: 32601882.
14. Liu H, Xie J, Fan L, et al. Cryptotanshinone protects against PCOS-induced damage of ovarian tissue via regulating oxidative stress, mitochondrial membrane potential, inflammation, and apoptosis via regulating ferroptosis. Oxid Med Cell Longev. 2022; 2022: 8011850, doi: 10.1155/2022/8011850, indexed in Pubmed: 35419170.
15. Shi D, Li H, Zhang Z, et al. Cryptotanshinone inhibits proliferation and induces apoptosis of breast cancer MCF-7 cells via GPER mediated PI3K/AKT signaling pathway. PLoS One. 2022; 17(1): e0262389, doi: 10.1371/journal.pone.0262389, indexed in Pubmed: 35061800.
16. Vundavilli H, Datta A, Sima C, et al. Anti-tumor effects of cryptotanshinone (C(19)H(20)O(3)) in human osteosarcoma cell lines. Biomed Pharmacother. 2022; 150: 112993, doi: 10.1016/j.biopha.2022.112993, indexed in Pubmed: 35462337.
17. Bahn G, Jo DG. Therapeutic approaches to alzheimer's disease through modulation of NRF2. Neuromolecular Med. 2019; 21(1): 1–11, doi: 10.1007/s12017-018-08523-5, indexed in Pubmed: 30617737.
18. Li C, Tang B, Feng Yu, et al. Pinostrobin exerts neuroprotective actions in neurotoxin-induced Parkinson's disease models through Nrf2 induction. J Agric Food Chem. 2018; 66(31): 8307–8318, doi: 10.1021/acs.jafc.8b02607, indexed in Pubmed: 29961319.
19. Cui Y, Ma S, Zhang C, et al. Pharmacological activation of the Nrf2 pathway by 3H-1, 2-dithiole-3-thione is neuroprotective in a mouse model of Alzheimer disease. Behav Brain Res. 2018; 336: 219–226, doi: 10.1016/j.bbr.2017.09.011, indexed in Pubmed: 28887195.
20. Cinegaglia N, Acosta-Navarro J, Rainho C, et al. Association of omnivorous and vegetarian diets with antioxidant defense mechanisms in men. J Am Heart Assoc. 2020; 9(12): e015576, doi: 10.1161/JAHA.119.015576, indexed in Pubmed: 32515251.
21. Zhang Q, Liu J, Duan H, et al. Activation of Nrf2/HO-1 signaling: an important molecular mechanism of herbal medicine in the treatment of atherosclerosis the protection of vascular

endothelial cells from oxidative stress. J Adv Res. 2021; 34: 43–63, doi: 10.1016/j.jare.2021.06.023, indexed in Pubmed: 35024180.
22. Bian Y, Chen Y, Wang X, et al. Oxyphylla A ameliorates cognitive deficits and alleviates neuropathology via the Akt-GSK3β and Nrf2-Keap1-HO-1 pathways in and in murine models of Alzheimer's disease. J Adv Res. 2021; 34: 1–12, doi: 10.1016/j.jare.2021.09.002, indexed in Pubmed: 35024177.
23. Fragoulis A, Schenkel J, Herzog M, et al. Nrf2 ameliorates DDC-induced sclerosing cholangitis and biliary fibrosis and improves the regenerative capacity of the liver. Toxicol Sci. 2019; 169(2): 485–498, doi: 10.1093/toxsci/kfz055, indexed in Pubmed: 30825315.
24. Taguchi K, Masui S, Itoh T, et al. Nrf2 activation ameliorates hepatotoxicity induced by a heme synthesis inhibitor. Toxicol Sci. 2019; 167(1): 227–238, doi: 10.1093/toxsci/kfy233, indexed in Pubmed: 30215777.
25. Yamamoto M, Kensler TW, Motohashi H. The KEAP1-NRF2 system: a thiol-based sensor-effector apparatus for maintaining redox homeostasis. Physiol Rev. 2018; 98(3): 1169–1203, doi: 10.1152/physrev.00023.2017, indexed in Pubmed: 29717933.
26. Liu FC, Chaudry IH, Yu HP. Hepatoprotective effects of corilagin following hemorrhagic shock are through Akt-dependent pathway. Shock. 2017; 47(3): 346–351, doi: 10.1097/SHK.0000000000000736, indexed in Pubmed: 27559697.
27. Liu FC, Liu FW, Yu HP. Ondansetron attenuates hepatic injury via p38 MAPK-dependent pathway in a rat haemorrhagic shock model. Resuscitation. 2011; 82(3): 335–340, doi: 10.1016/j.resuscitation.2010.11.007, indexed in Pubmed: 21168948.
28. El-Emam SZ, Soubh AA, Al-Mokaddem AK, et al. Geraniol activates Nrf-2/HO-1 signaling pathway mediating protection against oxidative stress-induced apoptosis in hepatic ischemia-reperfusion injury. Naunyn Schmiedebergs Arch Pharmacol. 2020; 393(10): 1849–1858, doi: 10.1007/s00210-020-01887-1, indexed in Pubmed: 32417955.
29. Lu WJ, Lin KH, Tseng MF, et al. New therapeutic strategy of hinokitiol in haemorrhagic shock-induced liver injury. J Cell Mol Med. 2019; 23(3): 1723–1734, doi: 10.1111/jcmm.14070, indexed in Pubmed: 30548082.
30. Hsieh YC, Yu HP, Suzuki T, et al. Upregulation of mitochondrial respiratory complex IV by estrogen receptor-beta is critical for inhibiting mitochondrial apoptotic signaling and restoring cardiac functions following trauma-hemorrhage. J Mol Cell Cardiol. 2006; 41(3): 511–521, doi: 10.1016/j.yjmcc.2006.06.001, indexed in Pubmed: 16859701.
31. Poulose N, Raju R. Aging and injury: alterations in cellular energetics and organ function. Aging Dis. 2014; 5(2): 101–108, doi: 10.14336/AD.2014.0500101, indexed in Pubmed: 24729935.
32. Wang H, Guan Y, Karamercan MA, et al. Resveratrol rescues kidney mitochondrial function following hemorrhagic shock. Shock. 2015; 44(2): 173–180, doi: 10.1097/SHK.0000000000000390, indexed in Pubmed: 25895148.
33. Mao Y, Qu Y, Wang Q. Cryptotanshinone reduces neurotoxicity induced by cerebral ischemia-reperfusion injury involving modulation of microglial polarization. Restor Neurol Neurosci. 2021; 39(3): 209–220, doi: 10.3233/RNN-201070, indexed in Pubmed: 34219678.
34. Wolf A, Thakral S, Mulier KE, et al. Evaluation of novel formulations of d-β-hydroxybutyrate and melatonin in a rat model of hemorrhagic shock. Int J Pharm. 2018; 548(1): 104–112, doi: 10.1016/j.ijpharm.2018.06.046, indexed in Pubmed: 29936200.
35. Nugent WH, Sheppard FR, Dubick MA, et al. Microvascular and systemic impact of resuscitation with pegylated carboxyhemoglobin-based oxygen carrier or hetastarch in a rat model of transient hemorrhagic shock. Shock. 2020; 53(4): 493–502, doi: 10.1097/SHK.0000000000001370, indexed in Pubmed: 31045989.
36. Wilfred BS, Madathil SK, Cardiff K, et al. Alterations in peripheral organs following combined hypoxemia and hemorrhagic shock in a rat model of penetrating ballistic-like brain injury. J Neurotrauma. 2020; 37(4): 656–664, doi: 10.1089/neu.2019.6570, indexed in Pubmed: 31595817.
37. Tomiyama K, Ikeda A, Ueki S, et al. Inhibition of Kupffer cell-mediated early proinflammatory response with carbon monoxide in transplant-induced hepatic ischemia/reperfusion injury in rats. Hepatology. 2008; 48(5): 1608–1620, doi: 10.1002/hep.22482, indexed in Pubmed: 18972563.
38. Kluck RM, Bossy-Wetzel E, Green DR, et al. The release of cytochrome c from mitochondria: a primary site for Bcl-2 regulation of apoptosis. Science. 1997; 275(5303): 1132–1136, doi: 10.1126/science.275.5303.1132, indexed in Pubmed: 9027315.
39. Yang J, Liu X, Bhalla K, et al. Prevention of apoptosis by Bcl-2: release of cytochrome c from mitochondria blocked. Science. 1997; 275(5303): 1129–1132, doi: 10.1126/science.275.5303.1129, indexed in Pubmed: 9027314.
40. Youle RJ, Strasser A. The BCL-2 protein family: opposing activities that mediate cell death. Nat Rev Mol Cell Biol. 2008; 9(1): 47–59, doi: 10.1038/nrm2308, indexed in Pubmed: 18097445.
41. Muñoz-Pinedo C, Guío-Carrión A, Goldstein JC, et al. Different mitochondrial intermembrane space proteins are released during apoptosis in a manner that is coordinately initiated but can vary in duration. Proc Natl Acad Sci U S A. 2006; 103(31): 11573–11578, doi: 10.1073/pnas.0603007103, indexed in Pubmed: 16864784.
42. Kinnally KW, Antonsson B. A tale of two mitochondrial channels, MAC and PTP, in apoptosis. Apoptosis. 2007; 12(5): 857–868, doi: 10.1007/s10495-007-0722-z, indexed in Pubmed: 17294079.
43. Sun F, Zhou Q, Pang X, et al. Revealing various coupling of electron transfer and proton pumping in mitochondrial respiratory chain. Curr Opin Struct Biol. 2013; 23(4): 526–538, doi: 10.1016/j.sbi.2013.06.013, indexed in Pubmed: 23867107.
44. Reisman SA, Buckley DB, Tanaka Y, et al. CDDO-Im protects from acetaminophen hepatotoxicity through induction of Nrf2-dependent genes. Toxicol Appl Pharmacol. 2009; 236(1): 109–114, doi: 10.1016/j.taap.2008.12.024, indexed in Pubmed: 19371629.
45. Xu W, Hellerbrand C, Köhler UA, et al. The Nrf2 transcription factor protects from toxin-induced liver injury and fibrosis. Lab Invest. 2008; 88(10): 1068–1078, doi: 10.1038/labinvest.2008.75, indexed in Pubmed: 18679376.
46. Battino M, Giampieri F, Pistollato F, et al. Nrf2 as regulator of innate immunity: A molecular Swiss army knife! Biotechnol Adv. 2018; 36(2): 358–370, doi: 10.1016/j.biotechadv.2017.12.012, indexed in Pubmed: 29277308.
47. Thimmulappa RK, Lee H, Rangasamy T, et al. Nrf2 is a critical regulator of the innate immune response and survival during experimental sepsis. J Clin Invest. 2006; 116(4): 984–995, doi: 10.1172/JCI25790, indexed in Pubmed: 16585964.
48. Kahroba H, Ramezani B, Maadi H, et al. The role of Nrf2 in neural stem/progenitors cells: From maintaining stemness and self-renewal to promoting differentiation capability and facilitating therapeutic application in neurodegenerative disease. Ageing Res Rev. 2021; 65: 101211, doi: 10.1016/j.arr.2020.101211, indexed in Pubmed: 33186670.
49. Saji N, Francis N, Blanchard CL, et al. Rice bran phenolic compounds regulate genes associated with antioxidant and anti-inflammatory activity in human umbilical vein endothelial cells with induced oxidative stress. Int J Mol Sci. 2019; 20(19), doi: 10.3390/ijms20194715, indexed in Pubmed: 31547608.
50. Kudoh K, Uchinami H, Yoshioka M, et al. Nrf2 activation protects the liver from ischemia/reperfusion injury in mice. Ann Surg.

2014; 260(1): 118–127, doi: 10.1097/SLA.0000000000000287, indexed in Pubmed: 24368646.
51. Zheng Yi, Tao S, Lian F, et al. Sulforaphane prevents pulmonary damage in response to inhaled arsenic by activating the Nrf2-defense response. Toxicol Appl Pharmacol. 2012; 265(3): 292–299, doi: 10.1016/j.taap.2012.08.028, indexed in Pubmed: 22975029.
52. Lin W, Wu RT, Wu T, et al. Sulforaphane suppressed LPS-induced inflammation in mouse peritoneal macrophages through Nrf2 dependent pathway. Biochem Pharmacol. 2008; 76(8): 967–973, doi: 10.1016/j.bcp.2008.07.036, indexed in Pubmed: 18755157.
53. Jiang Xi, Hu Y, Zhou Y, et al. Irisin protects female mice with LPS-induced endometritis through the AMPK/NF-κB pathway. Iran J Basic Med Sci. 2021; 24(9): 1247–1253, doi: 10.22038/ijbms.2021.56781.12678, indexed in Pubmed: 35083012.
54. Hsu JT, Kuo CJ, Chen TH, et al. Melatonin prevents hemorrhagic shock-induced liver injury in rats through an Akt-dependent HO-1 pathway. J Pineal Res. 2012; 53(4): 410–416, doi: 10.1111/j.1600-079X.2012.01011.x, indexed in Pubmed: 22686283.
55. Matsiukevich D, Piraino G, Lahni P, et al. Metformin ameliorates gender-and age-dependent hemodynamic instability and myocardial injury in murine hemorrhagic shock. Biochim Biophys Acta Mol Basis Dis. 2017; 1863(10 Pt B): 2680–2691, doi: 10.1016/j.bbadis.2017.05.027, indexed in Pubmed: 28579457.
56. 56. Kensler TW, Wakabayashi N, Biswal S. Cell survival responses to environmental stresses via the Keap1-Nrf2-ARE pathway. Annu Rev Pharmacol Toxicol. 2007; 47: 89–116, doi: 10.1146/annurev.pharmtox.46.120604.141046, indexed in Pubmed: 16968214.
57. McGrath-Morrow S, Lauer T, Yee M, et al. Nrf2 increases survival and attenuates alveolar growth inhibition in neonatal mice exposed to hyperoxia. Am J Physiol Lung Cell Mol Physiol. 2009; 296(4): L565–L573, doi: 10.1152/ajplung.90487.2008, indexed in Pubmed: 19151108.
58. Zoja C, Benigni A, Remuzzi G. The Nrf2 pathway in the progression of renal disease. Nephrol Dial Transplant. 2014; 29 Suppl 1: i19–i24, doi: 10.1093/ndt/gft224, indexed in Pubmed: 23761459.

Submitted: 2 December, 2022
Accepted after reviews: 12 June, 2023
Available as AoP: 21 June, 2023